

# Identified charged hadron production at high $p_T$ in $\sqrt{s_{NN}} = 200$ GeV Au + Au collisions at RHIC-PHENIX

M. Konno<sup>a</sup> for the PHENIX Collaboration

Graduate School of Pure and Applied Sciences, University of Tsukuba, Tsukuba, Ibaraki 305-8571, Japan

Received: 6 August 2006 /

Published online: 27 October 2006 – © Springer-Verlag / Società Italiana di Fisica 2006

**Abstract.** Identified hadron analyses in heavy ion collisions at RHIC show particle-type dependences of hadron yields, especially a baryon/meson difference at intermediate  $p_T$  (2–5 GeV/ $c$ ). In  $\sqrt{s_{NN}} = 200$  GeV Au + Au collisions, there is a significant suppression in meson yields compared to expectations from scaled  $p + p$  results. In contrast, a large enhancement of baryons relative to mesons is observed at intermediate  $p_T$ . The  $p_T$  reach of charged hadron identification has been extended by high statistics Au + Au data and the introduction of an aerogel Cherenkov detector. We can now study the identified charged hadron production at higher  $p_T$  using the PHENIX detector. In this paper, we present identified charged hadron  $p_T$  spectra, particle ratios, nuclear modification factors in Au + Au collisions at  $\sqrt{s_{NN}} = 200$  GeV.

**PACS.** 25.75.Dw; 25.75.-q

## 1 Introduction

Identified hadron analyses in heavy ion collisions at RHIC show particle-type dependences of hadron yields, especially a baryon/meson difference at intermediate  $p_T$  (2–5 GeV/ $c$ ). In central Au + Au collisions at  $\sqrt{s_{NN}} = 200$  GeV, there is a significant suppression in meson yields ( $\pi$ ,  $K$ , etc.) compared to peripheral Au + Au or  $p + p$  results. In contrast, a large enhancement of baryons ( $p$ ,  $\bar{p}$ ,  $\Lambda$ , etc.) relative to mesons is observed at intermediate  $p_T$  [1–4]. In this  $p_T$  region, jet fragmentation process dominates the hadron production in  $p + p$  collisions. And we expect that the fragmentation is independent of the collision system. Therefore the large baryon fraction observed at RHIC is one of the surprising findings. By performing a control experiment –  $d + Au$  collisions, in which only cold nuclear matter is produced, we found that the suppression of hadron yields is not caused by initial state interactions, but by final state interactions (i.e. jet quenching) [5]. We also found that the Cronin effect (enhancement from multiple scattering) has a particle-type dependence. The Cronin effect is larger for protons than those for pions, kaons. But, this difference between baryons and meson is not enough to account for the baryon enhancement seen in Au + Au collisions [6].

The observed baryon enhancement is explained in some different ways: (1) strong radial flow which pushes the heavier particles to larger  $p_T$  [7], (2) recombination of hard-scattered quarks with quarks from the thermalized medium [8–10], etc. On the other hand, in elliptic flow

measurements, a baryon/meson difference is also found in its magnitude ( $v_2$  as a function of  $p_T$ ). Moreover, by scaling with the number of constituent quarks, we obtain a common  $v_2$  curve for any particle types [11]. This scaling feature supports the quark recombination picture for the hadron production at RHIC. Recently the intermediate  $p_T$  region is considered a transition region from soft to hard hadron production mechanisms. Here, soft part includes hydrodynamic flow, quark recombination, etc. and hard part includes jet fragmentation which is well described by pQCD calculation. We expect to observe a transition from soft to hard hadron production in this  $p_T$  region.

In the PHENIX experiment, the  $p_T$  reach of charged hadron identification has been extended by high statistics Au + Au data and the introduction of a new aerogel Cherenkov detector. We can now study the identified charged hadron production at higher  $p_T$  using the PHENIX detector. A detailed study of identified hadron spectra and yields in this  $p_T$  region could be effective to understand multiple hadron production mechanisms as mentioned above. In this paper, we present identified charged hadron  $p_T$  spectra, particle ratios, nuclear modification factors in Au + Au collisions at  $\sqrt{s_{NN}} = 200$  GeV.

## 2 Data analysis

Data sets used here are Au + Au collisions at  $\sqrt{s_{NN}} = 200$  GeV and 62.4 GeV taken in RHIC Run4. Events with

<sup>a</sup> e-mail: konno@rcf.rhic.bnl.gov

a vertex position along the beam axis within  $|z| < 30$  cm were triggered by the beam-beam counters (BBC) located at  $|\eta| = 3.0-3.9$ . The Au + Au minimum bias data sample is subdivided into different centrality bins, where a collision centrality is determined from the charged particle multiplicity measured by the BBC. Charged particle tracks are reconstructed at mid-rapidity  $|\eta| < 0.35$  using a drift chamber and multi-wire proportional chambers with pad readout. Particle identification is performed with a time-of-flight detector and an aerogel Cherenkov detector. The time-of-flight detector has a timing resolution of  $\sim 120$  ps. The particle identification is based on particle mass calculated from the measured momentum, the velocity obtained from time-of-flight and path length along the trajectory. The aerogel Cherenkov detector (having a refractive index of  $n \sim 1.011$ ) was installed just before Run4, and was started to take collision data from Run4. The  $p_T$  reach of particle identification is extended (up to 5 GeV/c for charged pions, and 6 GeV/c for (anti)protons) by the introduction of the aerogel Cherenkov detector. Corrections to the charged particle spectrum for geometrical acceptance, decay in flight, tracking efficiency, and momentum resolution are determined using a single-particle GEANT Monte Carlo simulation. Multiplicity-dependent corrections for the detection efficiencies are evaluated by embedding simulated tracks into real events. Once all correction factors are determined as a function of  $p_T$  and centrality, they are applied to the raw spectra to obtain the final ones.

No feed-down correction from weak decays is applied to the results presented in this paper.

### 3 Results

#### 3.1 $p_T$ spectra

Figures 1 and 2 are  $p_T$  spectra for charged pions and (anti)protons for different centralities in Au + Au collisions at  $\sqrt{s_{NN}} = 200$  GeV. The spectra are measured by the aerogel detector. No feed-down correction from weak decays is applied for the results.

#### 3.2 $p/\pi$ ratios

The  $p_T$  dependence of  $p/\pi$  ratios provides more insights to the baryon production. Figure 3 shows  $p/\pi^+$  ( $\bar{p}/\pi^-$ ) ratios as a function of  $p_T$  in minimum bias Au + Au collisions at  $\sqrt{s_{NN}} = 200$  GeV. After reaching a maximum at approximately 2–3 GeV/c, the ratios then decrease at higher  $p_T$  and looks to approach some constant values. Figure 4 shows the centrality dependence of  $p/\pi^+$  ( $\bar{p}/\pi^-$ ) ratios as a function of  $p_T$ . The  $p/\pi$  ratios in the intermediate  $p_T$  range show a centrality dependence with higher relative baryon production in more central collisions. In central collisions, the  $p/\pi$  ratio shows that approximately equal

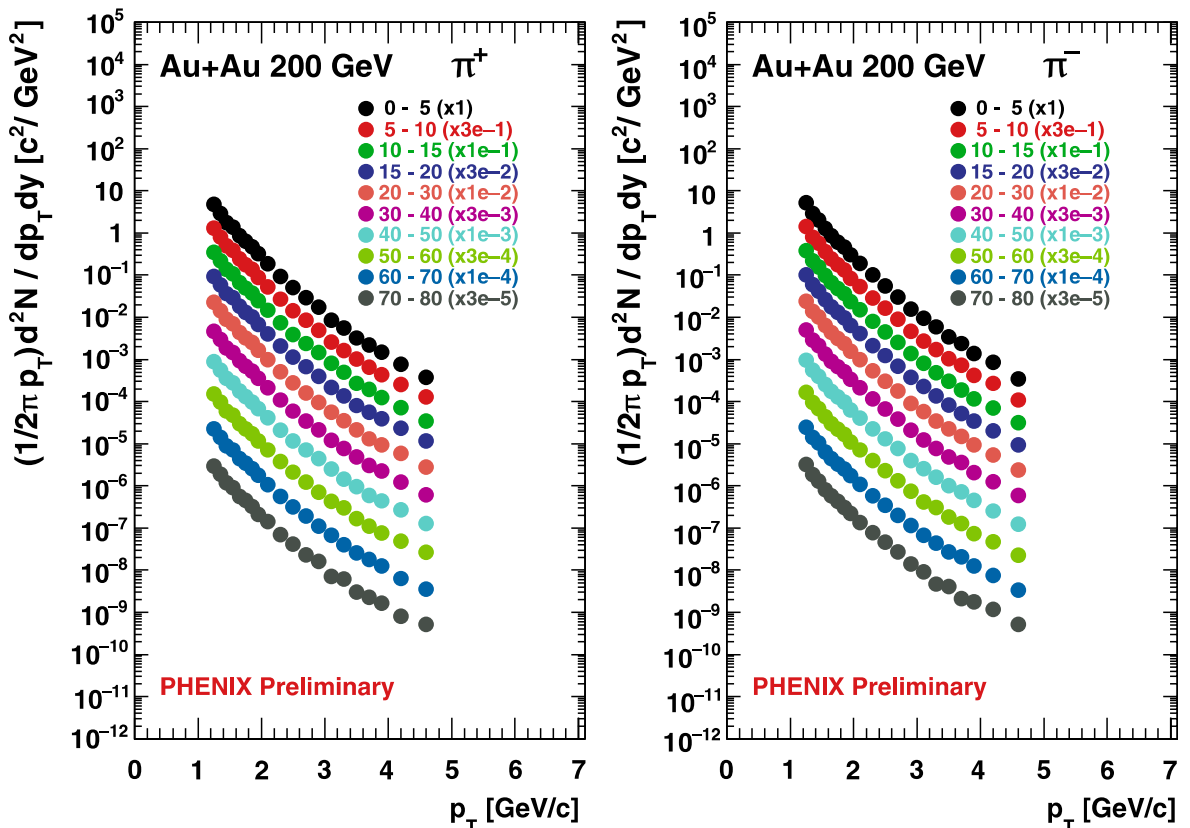
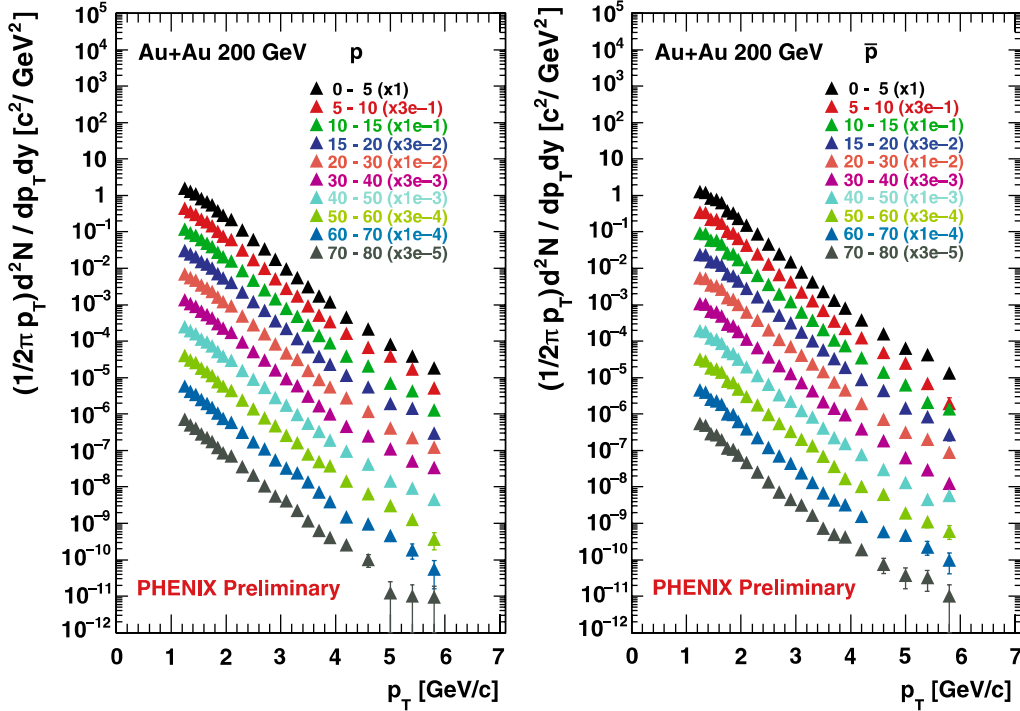
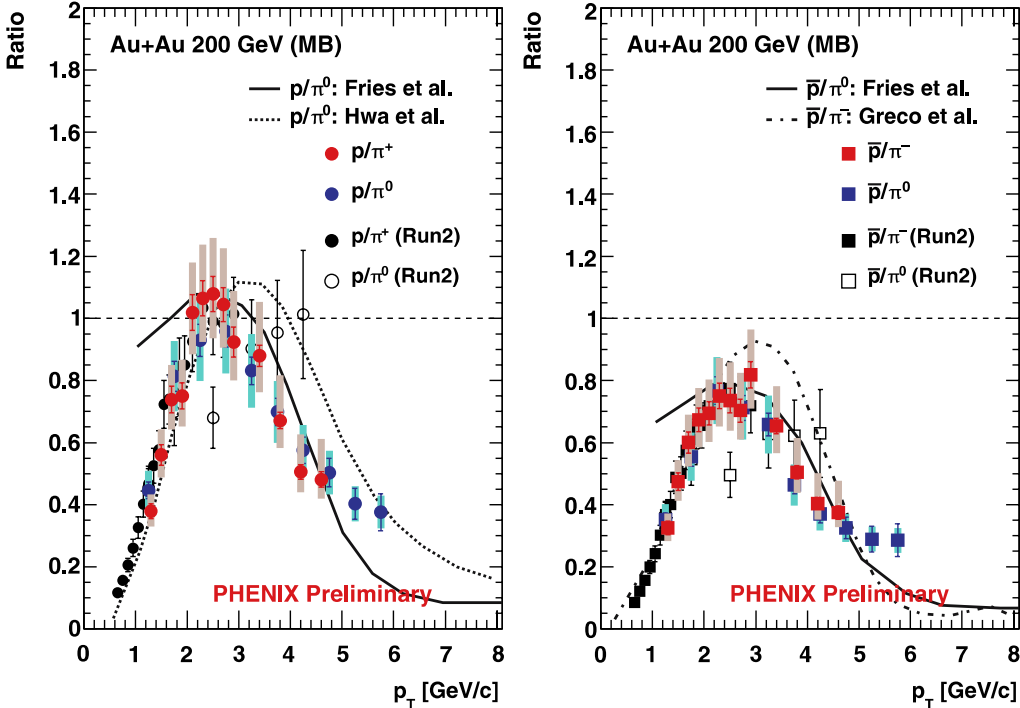


Fig. 1.  $p_T$  spectra for charged pions for different centralities in Au + Au collisions at  $\sqrt{s_{NN}} = 200$  GeV



**Fig. 2.**  $p_T$  spectra for protons and antiprotons for different centralities in Au+Au collisions at  $\sqrt{s_{NN}} = 200$  GeV. Note that no feed-down correction for weak decays is applied



**Fig. 3.**  $p/\pi^+$  (left) and  $\bar{p}/\pi^-$  (right) ratios as a function of  $p_T$  in minimum bias Au+Au collisions at  $\sqrt{s_{NN}} = 200$  GeV. Note that no feed-down correction for weak decays is applied. Curves show various model predictions [8–10]

amounts of protons and pions are produced in the momentum range of  $p_T = 1.5\text{--}3.5$  GeV/ $c$ . This is significantly higher than the results in elementary collisions ( $p+p$ ,  $e^+ + e^-$ ) or pQCD calculations,  $p/\pi \sim 0.2$  [8–10, 12, 13]. A definite turnover is observed for all centrality classes. The peak position is at 2–3 GeV/ $c$  independent of centrality. Beyond the peak, the ratios are falling toward the values in  $p+p$  collisions, though with the current limited statistics no conclusion can be drawn whether the ratios at high  $p_T$  in

Au+Au are the same as in  $p+p$ . Au+Au collisions indicate that the dominant source of hadron production in this  $p_T$  range is not jet fragmentation in vacuum. Theoretical model calculations for  $p/\pi$  ratios [8–10] are compared to the experimental data in Fig. 3. These models are similar in that they subscribe to a recombination process of quarks, but they have different implementations. Quark recombination models qualitatively describe the observed ratios.

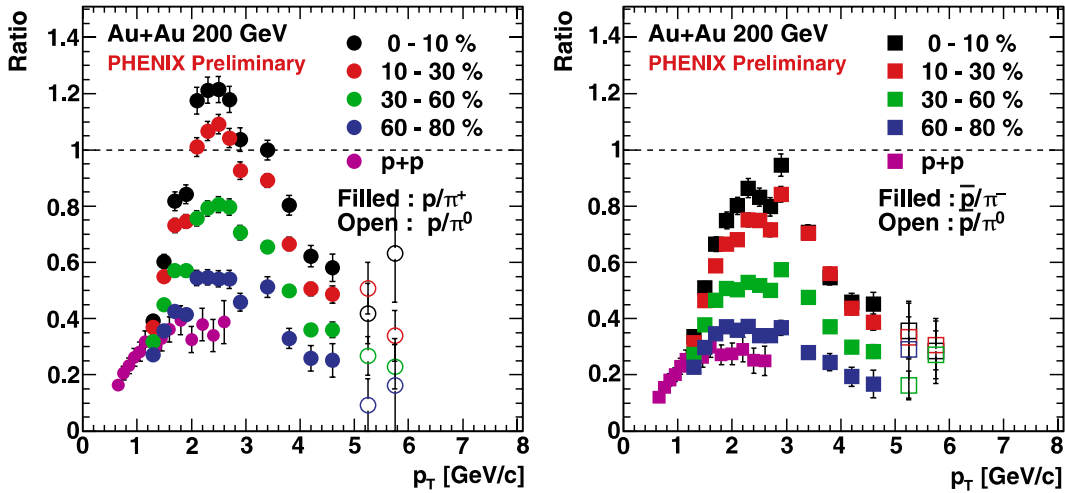


Fig. 4.  $p/\pi^+$  (left) and  $\bar{p}/\pi^-$  (right) ratios as a function of  $p_T$  for different centralities in Au + Au collisions at  $\sqrt{s_{NN}} = 200$  GeV. Note that no feed-down correction for weak decays is applied

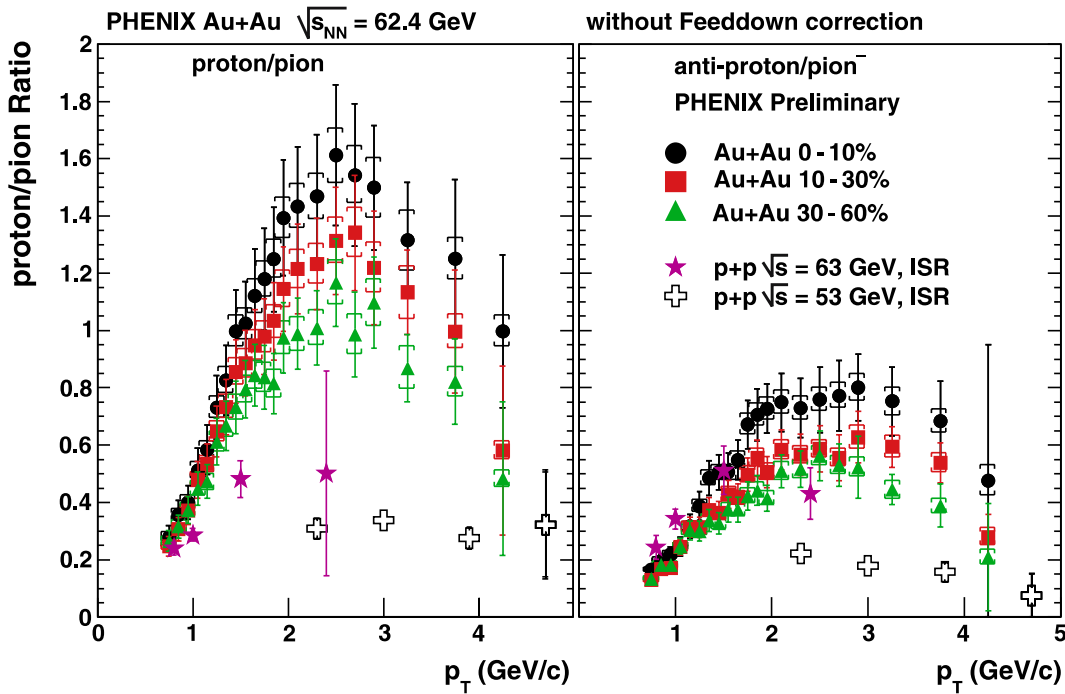


Fig. 5.  $p/\pi^+$  (left) and  $\bar{p}/\pi^-$  (right) ratios as a function of  $p_T$  for different centralities in Au + Au collisions at  $\sqrt{s_{NN}} = 62.4$  GeV. Note that no feed-down correction for weak decays is applied

The lower energy data provides an important information on the baryon production and transport at mid-rapidity between SPS and RHIC. Figure 5 shows the  $p/\pi^+$  ( $\bar{p}/\pi^-$ ) ratios as a function of  $p_T$  in Au + Au collisions at  $\sqrt{s_{NN}} = 62.4$  GeV. The ratios show a peak structure around 2–3 GeV/c and a centrality dependence as seen at  $\sqrt{s_{NN}} = 200$  GeV. Comparing to the 200 GeV data, the 62.4 GeV data shows a slightly larger proton contribution at intermediate  $p_T$ , while there is a less antiproton contribution. These observations may be related to the following differences: (1) larger difference between the slopes of spectra from fragmentation and recombination processes at 62.4 GeV than that at 200 GeV [14], (2) larger baryon chemical potential at 62.4 GeV than that at 200 GeV, or (3) stronger transport of baryon number from the incoming beams to midrapidity at lower energy.

### 3.3 $\bar{p}/p$ ratios

Figures 6 and 7 show  $\bar{p}/p$  ratio for minimum bias and centrality selected data respectively in Au + Au collisions at  $\sqrt{s_{NN}} = 200$  GeV. The ratio is almost independent of  $p_T$  and centrality up to 6 GeV/c. Theoretical pQCD calculations predict a decrease in the ratio over all  $p_T$  [15, 16]. In contrast, the measured ratio does not show such a clear decreasing trend. This observation indicates an importance of non-perturbative effects in baryon production even at  $p_T = 6$  GeV/c.

### 3.4 Nuclear modification factor ( $R_{CP}$ )

To look at the centrality dependence on the spectra in detail, it is useful to calculate the nuclear modification factor.

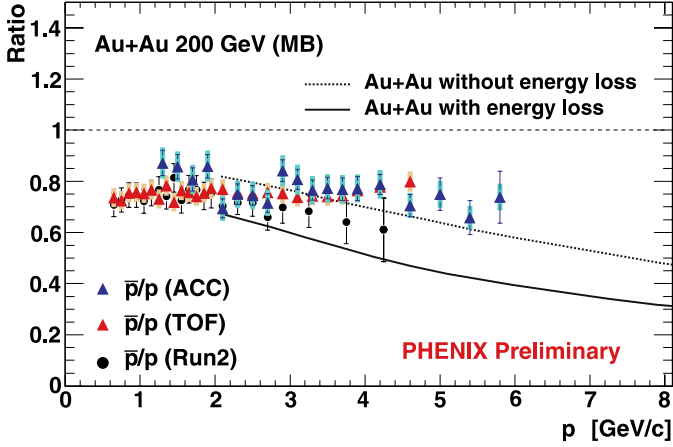


Fig. 6.  $\bar{p}/p$  ratio as a function of  $p_T$  in minimum bias Au + Au collisions at  $\sqrt{s_{NN}} = 200$  GeV. Note that no feed-down correction for weak decays is applied. Curves are the predictions from a jet quenching model [15, 16]

The nuclear modification factor  $R_{CP}$  is the ratio of  $N_{\text{binary}}$ -scaled spectra of central to peripheral Au + Au collisions.  $N_{\text{binary}}$  is the number of binary collisions for each centrality bin evaluated by a Glauber Monte Carlo calculation. Figure 8 shows the nuclear modification factor  $R_{CP}$  for pions, kaons and (anti)protons in 0%–10% central collisions

normalized by peripheral 60%–80% collisions. The overall systematic error ( $N_{\text{binary}}$  uncertainties) on  $R_{CP}$  is shown as a vertical band. The statistical errors are shown as an error bar on each data point. For the proton  $R_{CP}$ , the statistical errors has been significantly reduced compared to Run2 results by the high statistics data and the introduction of the aerogel detector. The result shows a stronger suppression for pions than protons in the intermediate  $p_T$  range. In this  $p_T$  region, where jet fragmentation dominates for the hadron production, one should expect similar values of  $R_{CP}$  for pions and protons if parton energy loss is the same. But we do not see such a tendency for the values of  $R_{CP}$  to approach each other at least up to 5 GeV/c. This means that soft hadron production like quark recombination may still be significant even at this  $p_T$ . Over the measured  $p_T$  range, we do not observe a difference in  $R_{CP}$  between particles and antiparticles. In 2005, the PHENIX experiment has collected the high statistics  $p + p$  data at  $\sqrt{s} = 200$  GeV. The data can be used as a reference to obtain the nuclear modification factor  $R_{AA}$  at high  $p_T$ .

## 4 Summary

Results on identified hadron production in Au + Au collisions at  $\sqrt{s_{NN}} = 200$  GeV are presented. The results are

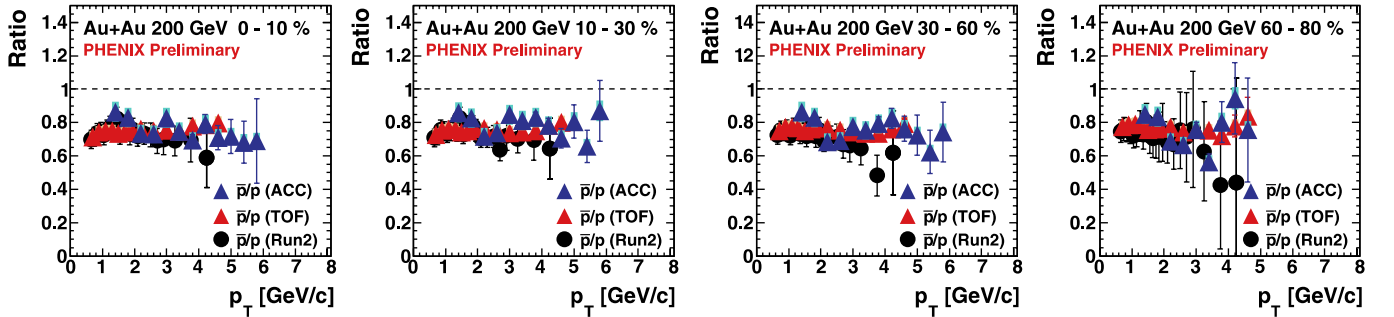


Fig. 7.  $\bar{p}/p$  ratio as a function of  $p_T$  for different centralities in Au + Au collisions at  $\sqrt{s_{NN}} = 200$  GeV. Note that no feed-down correction for weak decays is applied

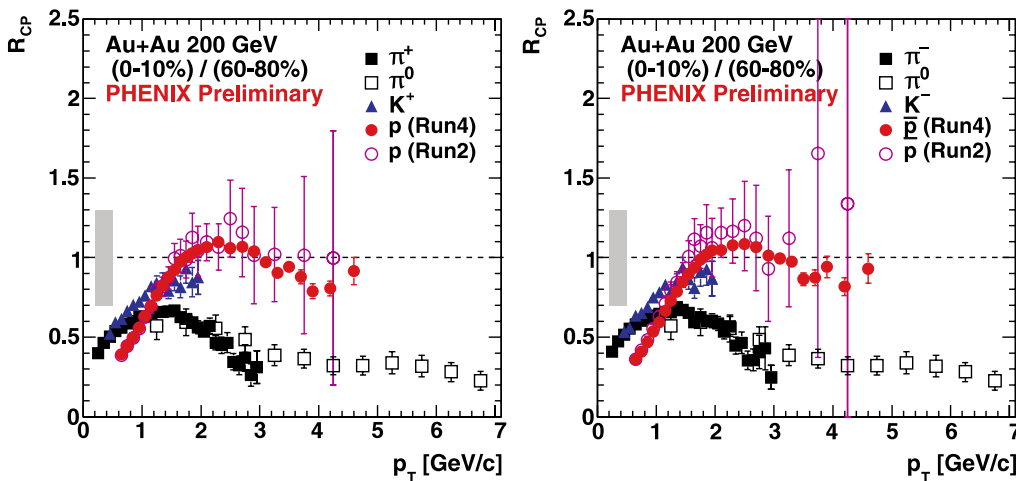


Fig. 8. Nuclear modification factor  $R_{CP}$  for pions, kaons, and (anti)protons. Note that no feed-down correction for weak decays is applied

obtained with the high statistics Au + Au data and the new aerogel Cherenkov detector. The baryon enhancement at intermediate  $p_T$  (2–5 GeV/ $c$ ) is confirmed again with a small statistical error and an extended  $p_T$  reach. The measured features at intermediate  $p_T$  are consistent with the thought that there are multiple hadron production mechanisms including both soft (quark recombination) and hard (jet fragmentation with parton energy loss) parts. Based on the observations: (1) baryon enhancement and (2) constituent-quark-number scaling of  $v_2$ , quark recombination process is thought to be a dominant hadron production mechanism in this  $p_T$  range. Soft part of hadron production extends to this  $p_T$  region in heavy ion collisions at RHIC. We also observe an indication of a transition from soft to hard hadron production in the  $p/\pi$  ratio. Comparing to the 200 GeV data, the 62.4 GeV Au + Au data shows a slightly larger proton contribution at intermediate  $p_T$ , while there is a less antiproton contribution. Different explanations of these observations are possible, for example, the larger difference between the slopes of spectra from fragmentation and recombination processes at 62.4 GeV than that at 200 GeV. A new time-of-flight detector, based on multi-gap resistive plate chambers, has been installed in Summer 2006. Together with the existing aerogel detector, we are now able to study the hadron production at high  $p_T$  with high precision in the future RHIC runs.

## References

1. PHENIX Collaboration, S.S. Adler et al., Phys. Rev. C **69**, 034910 (2004)
2. PHENIX Collaboration, S.S. Adler et al., Phys. Rev. Lett. **91**, 072301 (2003)
3. PHENIX Collaboration, S.S. Adler et al., Phys. Rev. C **69**, 034909 (2004)
4. STAR Collaboration, J. Adams et al., Phys. Rev. Lett. **92**, 052302 (2004)
5. PHENIX Collaboration, S.S. Adler et al., Phys. Rev. Lett. **91**, 072303 (2003)
6. PHENIX Collaboration, S.S. Adler et al., nucl-ex/0603010
7. T. Hirano, Y. Nara, Phys. Rev. C **69**, 034908 (2004)
8. R.J. Fries, B. Muller, C. Nonaka, S.A. Bass, Phys. Rev. C **68**, 044902 (2003)
9. R.C. Hwa, C.B. Yang, Phys. Rev. C **70**, 024905 (2004)
10. V. Greco, C.M. Ko, P. Levai, Phys. Rev. C **68**, 034904 (2003)
11. PHENIX Collaboration, M. Issah, A. Taranenko, nucl-ex/0604011
12. B. Alper et al., Nucl. Phys. B **100**, 237 (1975)
13. P. Abreu et al., Eur. Phys. J. C **17**, 207 (2000)
14. V. Greco, C. M. Ko, I. Vitev, Phys. Rev. C **71**, 041901 (2005)
15. X.N. Wang, Phys. Rev. C **58**, 2321 (1998)
16. I. Vitev, M. Gyulassy, Nucl. Phys. A **715**, 779 (2003)